

Article

Composite Cements Using Ground Granulated Blast Furnace Slag, Fly Ash, and Geothermal Silica with Alkali Activation

Andres Salas Montoya ¹, Loth I. Rodríguez-Barboza ^{2,*} , Fabiola Colmenero Fonseca ³ , Javier Cárcel-Carrasco ³ 
and Lauren Y. Gómez-Zamorano ^{2,*} 

¹ Departamento de Ingeniería Civil, Facultad de Ingeniería y Arquitectura, Universidad Nacional de Colombia, Manizales 170003, Colombia; asalasmo@unal.edu.co

² Programa Doctoral en Ingeniería de Materiales, Facultad de Ingeniería Mecánica y Eléctrica, Universidad Autónoma de Nuevo León, Ave. Universidad s/n, Ciudad Universitaria, San Nicolás de los Garza 66455, Nuevo León, Mexico

³ Instituto de Tecnología de Materiales, Universitat Politècnica de València, 46022 Valencia, Spain; fcolfon@upvnet.upv.es (F.C.F.); fracarc1@csa.upv.es (J.C.-C.)

* Correspondence: ivonnerodriguez.lirb@gmail.com (L.I.R.-B.); lauren.gomez@uanl.edu.mx (L.Y.G.-Z.)

Abstract: In recent decades, alkali activated and blended cements have attracted great interest worldwide due to their advantages of low energy cost, high strength, and good durability. This study evaluated the effects of replacing 50% of Portland cement with a mixture of three waste materials: ground granulated blast furnace slag (GGBFS), fly ash (FA), and geothermal waste (GS), with and without external alkaline activation, and activated with different alkali agents: 4 and 7% Na₂O equivalent of sodium hydroxide, sodium silicate (water glass), and sodium sulfate. After 90 days of curing, samples were characterized using compressive strength tests, scanning electron microscopy, X-ray diffraction, and thermogravimetric analyses. The results showed that sodium hydroxide caused an alkali–silica reaction and reduced the strength, while sodium silicate and sodium sulfate improved the strength and hydration products formation. Moreover, the addition of fly ash decreased the compressive strength but increased the workability, while the addition of slag and geothermal waste increased strength and densified the matrix with the formation of additional hydration products. The blended cements without activation also showed better performance than pure cement and a more compact matrix of hydration products. The study demonstrated the feasibility of using waste materials to produce blended cements with low energy costs and high durability.

Keywords: geothermal silica waste; composite cements; fly ash; ground granulated blast furnace slag



Citation: Salas Montoya, A.; Rodríguez-Barboza, L.I.; Colmenero Fonseca, F.; Cárcel-Carrasco, J.; Gómez-Zamorano, L.Y. Composite Cements Using Ground Granulated Blast Furnace Slag, Fly Ash, and Geothermal Silica with Alkali Activation. *Buildings* **2023**, *13*, 1854. <https://doi.org/10.3390/buildings13071854>

Academic Editor: Xiaoyong Wang

Received: 15 June 2023

Revised: 17 July 2023

Accepted: 18 July 2023

Published: 21 July 2023



Copyright: © 2023 by the authors. Licensee MDPI, Basel, Switzerland. This article is an open access article distributed under the terms and conditions of the Creative Commons Attribution (CC BY) license (<https://creativecommons.org/licenses/by/4.0/>).

1. Introduction

Portland cement concrete is the most widely used building material in the world, mainly because of its durability, strength, chemical stability, low production cost, and ability to be easily formed into a wide variety of shapes [1,2]. For all these reasons, the demand for concrete has increased with the progress and innovation of the construction industry, as there is no other material that can match its various properties [3,4]. However, the environmental impact has also increased, as the Portland cement (PC) industry is one of the main protagonists of the greenhouse effect and thus of global warming, due to the calcination of raw materials at temperatures above 1450 °C, which causes the emission of greenhouse gases such as CO₂, SO_x, and NO_x [5]. Due to the CO₂ emissions associated with cement production, currently reported around 7–9%, the need for environmentally friendly solutions for a reduction in the carbon footprint is currently an important research topic [1,6–8].

Innovations in Portland cement production processes have evolved to achieve better properties, reduce the environmental impact of the production process, and lower the cost of PC [9]. One of the most notable innovations is the use of composite cements, which are cements in which a portion of the Portland cement is replaced by industrial

by-products [10–12], including various types of pozzolanic and hydraulic materials [13,14]. Those cements have been used for several reasons, one of them is that these materials have shown highly desirable properties for certain purposes, such as delaying or reducing heat of hydration in massive structures, improving durability and, in some cases, achieving strengths above the normal range [15,16]. The use of alternative materials as a partial or total replacement of PC has represented an important advance in the construction industry, as a variety of by-product materials from different industries with high production volumes have been proposed with remarkable results. These materials have a promising future in the construction industry, not only as an ecological alternative, but also as a technological solution since the properties of those composite cements could be greatly improved [14]. However, with the current restrictions on the use of carbon due to policies or measures in several countries that have promoted the use of alternative energy and aimed at reducing the amount of carbon dioxide and other greenhouse gases emitted by human activities, the availability of such substitute mineral admixtures is beginning to decrease [5]. Therefore, it is imperative to search for SCMs in nature to expand the availability of these alternative materials.

Over the past few decades, there has been growing acknowledgment of the potential of aluminosilicate materials found in nature or generated as by-products in industries, such as fly ash (FA), ground granulated blast furnace slag (GGBFS), and metakaolin (MK). These materials have demonstrated their ability to serve as sustainable alternatives to ordinary Portland cement, leading to noteworthy environmental advantages [10,14,17]. Moreover, the use of geothermal silica (GS) has been reported by various researchers [18–20]. This is a by-product of the process of energy production by steam extraction from the subsurface. GS is obtained as a mixture of geothermal brine and steam that undergoes a series of steps to extract heat. The reports indicated that the GS has a strong pozzolanic behavior producing a densification of Portland cement hydration products matrix [18]. These benefits include reduced CO₂ emissions and energy consumption associated with Portland cement production, as well as the preservation of non-renewable natural resources [1,2,21–25]. Numerous studies have shown that these materials have practical utility as construction materials, particularly in the production of sustainable binders such as alkali-activated (AA) binders [17,24–35]. These binders offer several advantageous properties over ordinary Portland cement concrete (OPC). These include rapid high-strength development, excellent durability, and high resistance to temperature and chemical attacks [24,28,36,37]. Those benefits are attributed to the abundant availability of these materials and the presence of soluble silica and alumina in them [37,38]. Through the formation of reaction products and property development, these materials contribute to the strength and stability of these matrices [38].

The use of alkali-activated (AA) mortar or concrete has been steadily increasing in the construction industry. Extensive evaluations of AA binders, particularly those made from fly ash and ground granulated blast-furnace slag, have clearly demonstrated that these materials, which contain abundant amounts of silica (SiO₂), alumina (Al₂O₃), and/or calcium oxide (CaO), serve as suitable source materials. This is because the alkali activation process involves a chemical reaction between various aluminosilicate oxides and silicate, or the formation of a silica-rich calcium silicate hydrate (C-S-H) gel. These reactions contribute to a deeper understanding of these binder systems and their properties [32].

Recently, there have been reports on the development of hybrid cements that combine ordinary Portland cement (OPC) with alkali-activated cements [32]. These hybrid cements are obtained by blending OPC clinker in proportions of less than 30% by weight [34], together with supplementary cementitious materials (SCMs) in proportions of more than 70% by weight, and the addition of an activator in proportions of about 5% [29,39]. The importance of these mixtures, with their numerous advantages, has attracted considerable attention from the scientific and technological communities [29]. These mixtures show remarkable versatility, as they exploit the inherent properties of the raw materials used [29]. Hybrid cements have the advantage of accommodating significant amounts of mineral

admixtures, such as industrial by-products or natural pozzolans, which require alkaline activation. In addition, they require only small amounts of cement to facilitate the hardening of the mix when mixed with water. This has the notable advantage of reducing the clinker content in the mix, resulting in energy savings and conservation of natural resources. In the hydration process of hybrid cements based on GGBFS and PC, it has been observed that alkaline activation produces reaction products very similar to those formed during the hydration of conventional Portland cement. The primary reaction product formed is the C-A-S-H gel, which has a composition and structure different from the C-S-H gel formed by conventional Portland cement [35]. Furthermore, the hydration process of hybrid cements combining fly ash and Portland cement shows a different mechanism. FA, characterized by low CaO content and high SiO₂ and Al₂O₃ content, follows a model proposed by Palomo and Fernández-Jiménez [35,40]. This mechanism leads to alkaline activation, resulting in an amorphous matrix with cementitious properties, known as a N-A-S-H gel. In studies of supplementary cementitious materials (SCMs), researchers have observed the simultaneous formation of N-(C)-A-S-H, C-(N)-A-S-H, and C-A-S-H gels within the cementitious matrix. The specific types and amounts of precursors used contribute to the presence of these different gel formations [27,32,41,42].

Due to their high substitution content, this type of material must be combined with an alkaline solution for blending. Hybrid cements are included in the category of environmentally friendly cements since they combine the positive properties provided by an OPC with the properties of alkaline activated materials [41], generally resulting in a material with good mechanical properties [43]. Nevertheless, these hybrid cements are not well understood yet, and in order to see the effect of cement quantity on their properties, here is proposed up to 50% of replacement level.

With the aim of providing an alternative to the environmental impact caused by the production of PC and the growing demand for it, the main objective of the research was to evaluate composite pastes in which partial substitution of ordinary Portland cement (OPC) was made by a mixture of FA, GGBFS, and GS, with and without external alkaline activation utilizing water glass, sodium hydroxide and sodium sulfate, analyzing the compressive strength and the microstructures obtained. The formulations were prepared using different alkaline activators to improve the mechanical properties of the composite cements. The hydration products of the cements were then characterized to evaluate the interaction and hydration kinetics of the materials used at different curing ages. Consequently, the main novelty of this research is the comparison of the development of new composite cements containing different types of pozzolanic and hydraulic materials with and without alkaline activation.

2. Materials and Methods

The materials used in this investigation were: (a) *Alkaline activators*: Three different types of alkaline activators were used: (i) sodium hydroxide, (ii) Sodium silicate (water glass) with a ratio SiO₂/Na₂O = 2.0, and (iii) sodium sulfate. NaOH solutions with the required concentration were prepared by dissolving NaOH pellets in distilled water, leaving the solution to cool down for at least 24 h. Sodium hydroxide solution was used to adjust the Na₂O content in the activating solution. (b) *Precursors*: The materials used in this study were obtained from different suppliers in Mexico. A commercial Ordinary Portland cement (OPC), compatible with ASTM type I Portland cement, from Cemex Mexico was used for the mixes. In addition, ground granulated blast furnace slag (GGBFS) from the steel company Altos Hornos de México (AHMSA), fly ash (FA), and geothermal silica (GS), both from the Mexican Federal Electricity Commission, were used as supplementary cementitious materials (SCM).

The FA and GGBFS were sieved through a 75 µm mesh before use [25], with special care for geothermal waste; the GS is a material containing sodium and potassium chlorides, which must be removed by washing, as they can have a negative effect on the behavior of the replaced cement pastes. The treatment was carried out with potable water at 90 °C,

in a ratio of 3:1 water:GS; between each washing, a chloride analysis was carried out by titration. When the content was minimal (0.02%), the material was able to be used as a substitute for OPC [18]. The material was then dried at 110 °C for 24 h to remove all water. Table 1 lists some of the physical properties of the cementitious materials and shows that GGBFS and FA have the lowest Blaine fineness and GS has the highest, followed by OPC. The cementitious materials were also characterized by X-ray fluorescence spectroscopy and X-ray diffraction (XRD). Table 2 shows the chemical composition of the cementitious materials used in this research. Together with particle size, chemical composition is a key factor influencing the pozzolanic and hydraulic action of cementitious materials [44–46].

Table 1. Physical characteristics of cementitious materials used.

Cementitious Material/ Physical Characteristic	GGBFS	FA	GS	OPC
Specific gravity	2230	2080	2160	3050
Blaine fineness, (cm ² /g)	4948	4462	6652	5234
Median grain size, (µm)	0.1	17	19	15
Pozzolanic activity index	123	125	95	-

Table 2. Chemical compositions of cementitious materials used.

Oxide	GGBFS	FA	GS
SiO ₂	42.87	52.63	92.61
Al ₂ O ₃	9.0	22.75	-
Fe ₂ O ₃	0.58	6.38	-
K ₂ O	0.65	1.18	-
CaO	35.66	6.81	-
MgO	9.73	0.54	-
Na ₂ O	0.48	0.49	0.42

X-Ray diffraction patterns obtained from the precursors are shown in Figure 1. Figure 1 shows the diffraction pattern of the OPC, including its characteristic phases: alite, belite, aluminite, ferrite, and gypsum. The amount of each phase was calculated by Rietveld analysis and is shown in Table 3. GGBFS is a calcium silicoaluminate material which, due to its processing, tends to be highly vitreous [19], as can be seen from the diffraction pattern also in Figure 1; an important characteristic of this material is the appearance of an amorphous halo between 20°–40°2θ, it is also observed that it shows some weak reflections corresponding to akermanite, a typical phase of GGBFS. In the XRD pattern of the FA, the amorphous characteristics of aluminosilicates can be observed in 20 and 30°2θ, as well as the crystalline phases quartz, mullite, and calcite [15]. Additionally, the main characteristics of GS are published [13,15,47], showing only an amorphous halo between 20°–30°2θ. Moreover, for SCM, an amorphous structural state is generally required, i.e., with high internal energy and therefore thermodynamically unstable and highly chemically reactive [48,49]. The percentage of crystalline phases in the GGBFS and FA were analyzed using Rietveld, and the percentage of amorphous fraction was calculated by difference (see Tables 4 and 5). The amorphous properties of the materials used were within acceptable limits and that adequate cementitious properties can be expected [50].

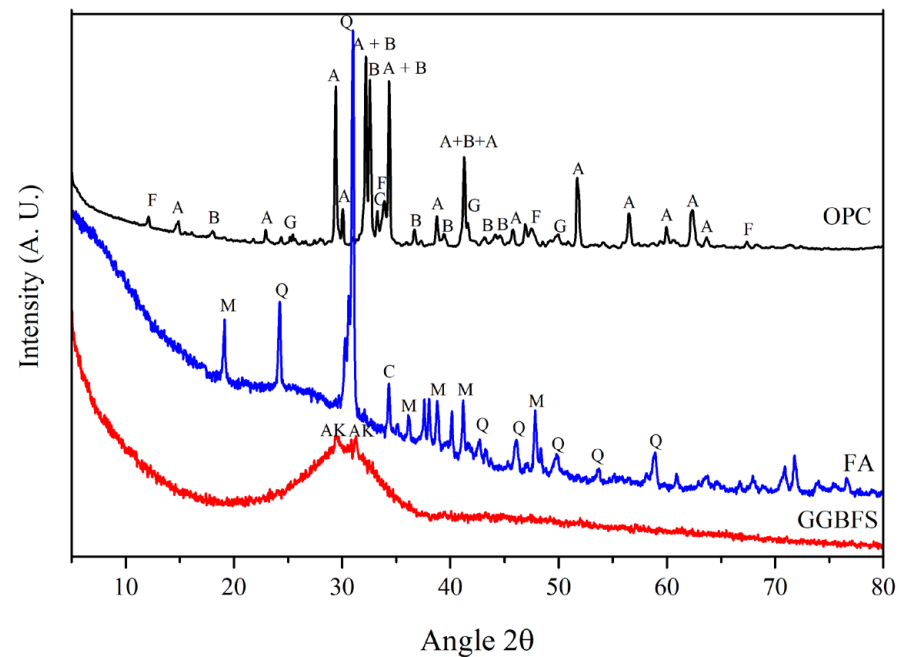


Figure 1. Diffraction pattern of: OPC, GGBFS, FA, where A = alite, B = belite, a = aluminate, F = ferrite, G = gypsum, AK = Akermanite, M = mullite, Q = Quartz, C = calcite.

Table 3. Phase composition of the OPC (Rietveld analysis).

Phase	%
Alite	44.03
Belite	16.14
Ferrite	6.41
Alum. cub	4.56
Alum ort.	0.11
Periclase	0.43
Arcanite	1.51
Portlandite	0.57
Calcite	24.63
Quartz	0.15
Gypsum	0.45
Free lime	0.0
TOTAL	98.99

Table 4. Results of the percentage of crystalline phase in GGBFS.

Phase	Chemical Formulae	% Crystalline Phase	Std. Error
Akermanite	$\text{Ca}_2\text{MgSi}_2\text{O}_7$	1	0.26
	Total	1	

Table 5. Results of the percentage of crystalline phases in FA.

Phase	Chemical Formulae	% Crystalline Phase	Std. Error
Quartz	SiO_2	15.93	0.35
Mullite	$\text{Al}_6\text{Si}_2\text{O}_{13}$	14.35	1.14
Calcite	CaCO_3	8.82	0.54
Hematite	Fe_2O_3	1.45	0.39
	Total	40.55	

The experimental program consisted of two stages (a) alkali-activated pastes prepared in the first stage, based on a 50% replacement of OPC with GGBFS, FA, and GS, and (b) 30% replacement without activation (see Table 6). The water/binder ratio was set at 0.4, giving good mechanical strength but poor workability, which was improved using polycarboxylate-based superplasticizer (SP) from Sika at a fixed proportion of 0.3% of the solids. The dosage of the alkaline activators was set to 4% and 7% of Na₂O equivalent (contained in) to sodium hydroxide, sodium silicate and sodium sulfate in order to avoid the low rate of setting time. Pastes without alkaline activation were prepared by adding distilled water and SP in a blender with a planetary movement and stirred during 30 s for complete incorporation. For the mixtures that required external alkaline activation with NaOH (NH), Na₂SiO₃ (SS), and Na₂SO₄ (NS), the activator was first dissolved in the water and the SP was added seconds before mixing to avoid degradation due to the high pH of the solution. The GS was mixed with the mixing water in the mixer at slow speed for 1 min and the OPC, GGBFS, and FA, previously dry homogenized, were added. Pastes were poured into cubic 50 mm plastic molds. The molds were vibrated on a vibrating table to eliminate any entrapped air, and then sealed with plastic film to prevent water evaporation during the first 24 h in a room at 20 ± 2 °C. Samples were cured under calcium hydroxide saturated water for up to 90 days. After reaching the respective curing age, compressive strength tests (CS) were performed following the ASTM C109 standard [51]; values were estimated from the average of four specimens. Then, fragments of the crushed specimens were submerged under acetone to stop the hydration reaction, during 72 h and dried at a vacuum oven at 40 °C for 24 h [52,53]. The dried samples were further ground in a zirconia mill, the resulting powder was sieved on a #200 mesh (74 µm) at various intervals until all the material passed through the mesh. The powder samples were used for X-ray diffraction (XRD), and thermogravimetric analysis (TGA). Some unground broken fragments were used for scanning electron microscopy (SEM) coupled with energy dispersive X-ray spectroscopy (EDS).

Table 6. Mixture design of composite cement mixtures.

Sample	OPC	GGBFS	FA	GS	Activation
100OPC	100	0	0	0	
50OPC-50GGBFS	50	50	0	0	4 and 7%Na ₂ O _{eq} of SS, NH and NS
50OPC-40GGBFS-5FA-5GS	50	40	5	5	4 and 7%Na ₂ O _{eq} of SS, NH and NS
50OPC-35GGBFS-10FA-5GS	50	35	10	5	4 and 7%Na ₂ O _{eq} of SS, NH and NS
50OPC-30GGBFS-10FA-10GS	50	30	10	10	4 and 7%Na ₂ O _{eq} of SS, NH and NS
50OPC-25GGBFS-15FA-10GS	50	25	15	10	4 and 7%Na ₂ O _{eq} of SS, NH and NS
70OPC-30GGBFS	70	30	0	0	
70OPC-10GGBFS-10FA-10GS	70	10	10	10	
50OPC-20GGBFS-10GS	70	20	0	10	

XRD analyses were performed on selected samples after 3 and 90 days of curing for OPC and activated composites and for 3 and 28 days of curing for non-activated composite cements and those activated with Na₂SO₄. XRD patterns were recorded on an Xpert MPD Phillips diffractometer using pure copper K-Alpha 1 radiation at a wavelength of 1.54 Å. The X-ray generator was operated at 40 kV and 40 mA. The settings were as follows: the recorded angular range was 10° to 90°(2θ) with a step close to 0.01°; step time 0.05 s and step size 0.01°. For the TGA samples of around 30 mg were heated from 25 to 950 °C at 10 °C/min in a nitrogen environment in a thermal analyzer. The mass loss at different temperatures was used to quantify the reaction product formation. SEM and EDS were performed to identify the changes in the microstructure and elemental composition of the selected samples. SEM images and EDS data were obtained on gold–palladium coated samples using a JEOL 6490 LV scanning electron microscope. The solid pieces of the selected pastes were mounted in epoxy resin, ground with SiC grit paper and then polished with diamond paste up to 0.25 microns. The accelerating voltage was set at 20 kV.

The characterization by EDS was performed by collecting 30 spot analyses per sample to determine the elemental analysis of the samples.

3. Results and Discussion

3.1. Compressive Strength

CS of neat OPC and composite cements with FA, GGBFS, and GS with different types of alkaline activations, cured up to 90 days, are shown in Figures 2–4 (see Tables S1 and S2 with all the measured data in a Supplementary File). It can be noted that all the blends showed a slower increase in strength in the early stages (3–14 days) compared to the OPC, which is a characteristic of several replaced cements as stated by Barnett et al. [49]. However, the SS and NS activated pastes met the strength specification for the type of OPC used (30 MPa strength at 28 days). For the NH activated compounds, there is a clear difference in the CS results. It has been reported that NH acts as an OPC retarder, in addition to the fact that activators have a selectivity characteristic [54] that depends on the composition of the materials used, and this may be directly related to the decrease in strength of such cements. Shi and Day [55] pointed out that in the case of alkali-activated cements based on GGBFS, there were important differences in CS activated with NH or SS, as well as with the type of GGBFS used, i.e., amorphous phase content and chemical composition, reporting better results with SS. In the case of cements activated with NH, none of the tests reached the compressive strength of 30 MPa.

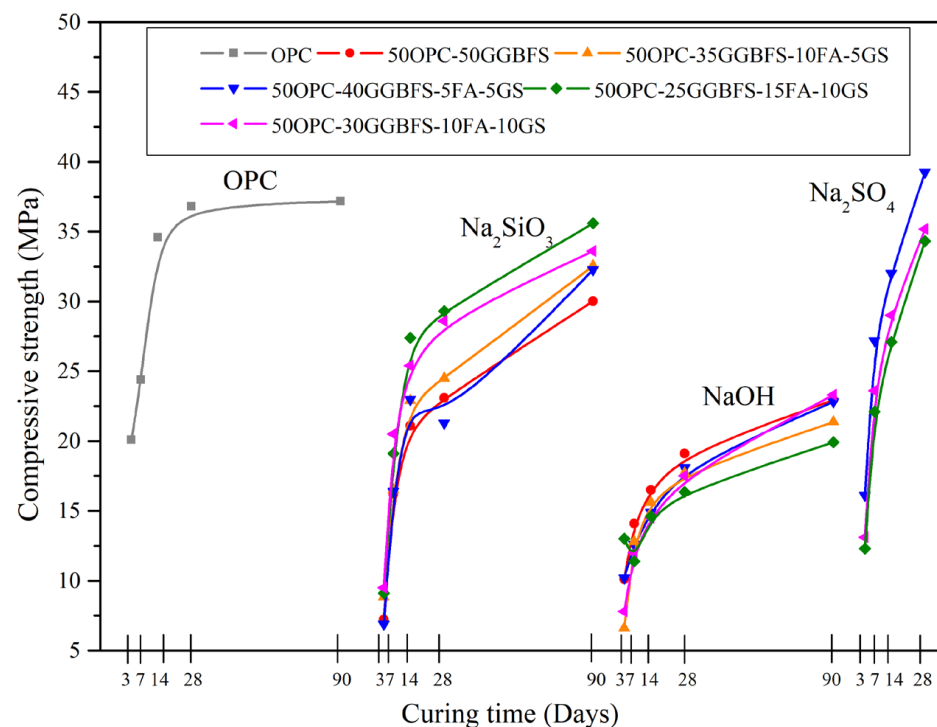


Figure 2. Compressive strength results vs. curing periods for all the composite cements activated with 4% of $\text{Na}_2\text{O}_{\text{eq}}$ of SS, NH, and NS, compared to OPC.

The results of the mixtures with NS shown in Figure 2 indicate a significant improvement in CS, as they not only meet the minimum strength expected for OPC, but also exceed it with strength increases of about 7%, showing higher strengths than those of the mixtures activated with SS. The increase in CS after 28 days for the NS activated cementitious composites with respect to the minimum strength of 30 MPa required for an OPC were 30.83% for the 50OPC-40GGBFS-5FA-5GS mix, 17.3% for the 50OPC-30GGBFS-10FA-10GS, and 14.36% for the 50OPC-25GGBFS-15FA-10GS.

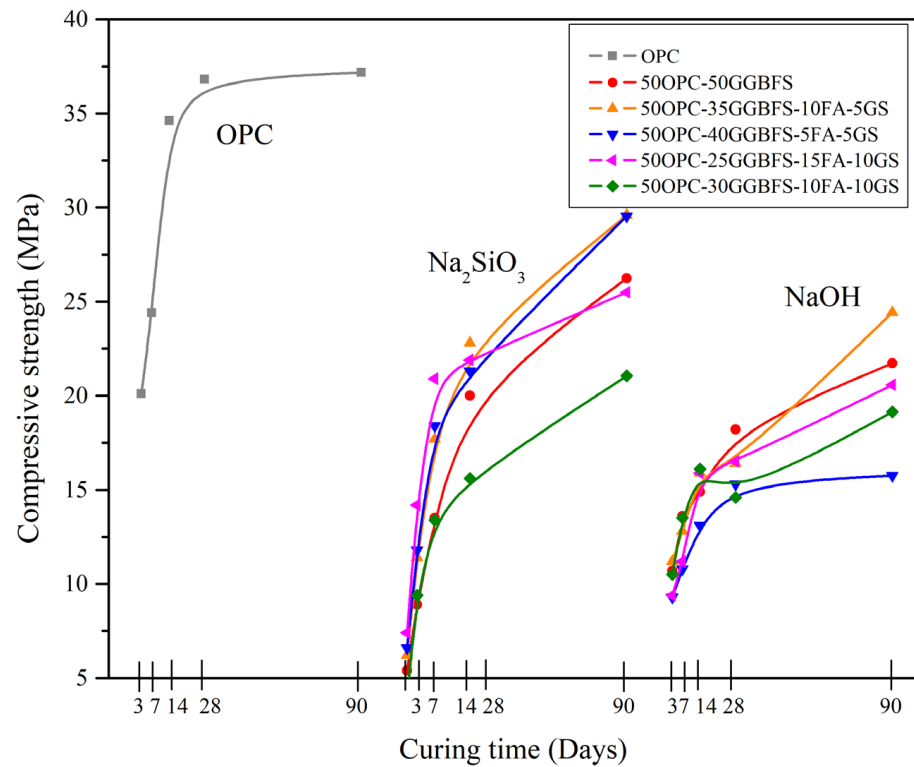


Figure 3. Compressive strength results vs. curing periods for all the composite cements activated with 7% of $\text{Na}_2\text{O}_{\text{eq}}$ of SS, NH, and NS, compared to OPC.

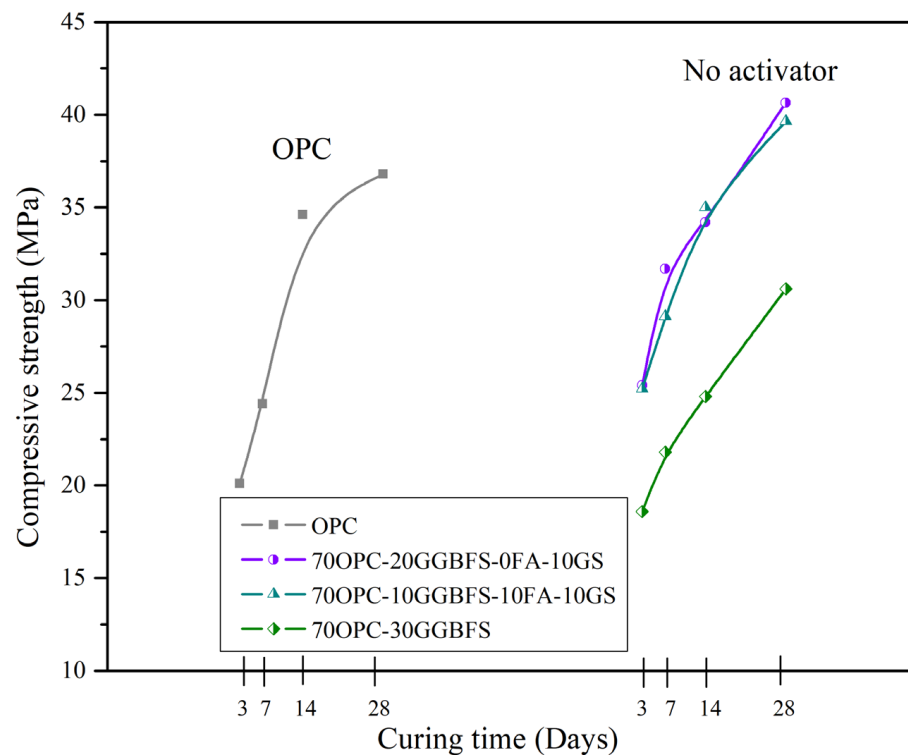


Figure 4. Compressive strength results vs. curing periods for all the composite cements without activation, compared to OPC.

Moreover, comparing both figures showed that the increase in the amount of FA in the SS activated systems decreased the CS of the composites due to a lack of interaction of this

material with the alkaline activators. Similarly, the use of high levels of GGBFS and GS also caused a decrease in CS; however, the higher mechanical properties were obtained when an intermediate level (50OPC-25GGBFS-15FA-10GS) was used. On the contrary, in the blends activated with NS, there is a clear improvement in the properties of the composites when there is a high proportion of GGBFS and with low amounts of FA and GS. In this case, a possible FA filler and the creation of nucleation sites by GS due to its nanometer particle size could have contributed to obtain a denser and more resistant hydration product matrix. To evaluate the effect of the amount of activator, the percentage of $\text{Na}_2\text{O}_{\text{eq}}$ was increased to 7% and the results of the CS are shown in Figure 3.

The compressive strength (CS) results obtained from an alkaline activation process with 7% $\text{Na}_2\text{O}_{\text{eq}}$ showed lower values compared to those obtained with pure ordinary Portland cement (OPC) at all curing times, as shown in Figure 3. This observation suggests that the activators used may have a detrimental interaction with the OPC particles [56]. In addition, the inadequate presence of activators may also affect the substitute materials. While previous studies have reported that activation with NH can yield higher strengths than OPC within a short hydration period, this phenomenon was not observed in the current research due to the formation of detrimental phases in the presence of the activators. This issue will be further discussed in the SEM section. The systems activated with SS showed slightly higher strengths than those activated with NH; however, for practical purposes, it is not feasible to activate the composites with such high activator concentrations since there is no significant increase in strength. As pointed out above, there is a better interaction of GGBFS with SS, but the presence of higher amount of FA and GS reduced the CS. When using NH there was no significant improvement in strength even at later ages, especially for the systems with high percentages of FA and GS; in the case of FA there was no apparent interaction with the activator and GS formed phases with a different composition from C-S-H, as will be seen later in SEM section, and reported elsewhere for alkaline activated materials.

To compare the results of the chemically activated blends, we investigated formulations with 30% OPC replacement without external alkaline activation (see Table 6). The CS results obtained from the 70OPC-30GGBFS system showed relatively low strength values when compared to 100OPC pastes as shown in Figure 4, this is due to the fact that GGBFS reacts slowly as reported in other investigations [31,57,58]; a basic characteristic of GGBFS is that it significantly improves CS at late ages, which is also evident in the GGBFS curve, so it is expected that the strength will be improved with longer hydration times. Although the rate of strength development of these systems is low, the minimum strength required for the type of cement used is achieved at 28 days. Nevertheless, 70OPC-10GGBFS-10FA-10GS and 70OPC-20GGBFS-10GS composite cements showed a significant improvement in CS with an increase of 7.75% and 10%, respectively, compared to the values achieved by 100OPC. When comparing the results to the minimum 28-day strength specification for OPC (30 MPa), the 70OPC-10GGBFS-10FA-10GS system showed an increase of 32.16% and the 70OPC-20GGBFS-10GS system of 35.5%. The above is attributed to the pozzolanic and latent hydraulic behavior of GS and GGBFS, respectively. Additionally, it has been reported that the SCM particles could act as nucleation sites, promoting the formation of the C-S-H gel, as well as densifying the cementitious matrix reducing the porosity (microfiller effect), the additional C-S-H formation through the pozzolanic reaction of all the SCM, and the improving on the flowability through the FA effect, also reduced the porosity [22,59].

3.2. X-ray Diffraction

Figures 5 and 6 show the XRD patterns of selected alkali activated composite samples cured at 3 and 28 days compared with neat OPC. In the OPC pattern are observed the main phases of a cement composed of alite, belite, ferrite, calcite, as well as some of the hydration products, which include portlandite (CH) and ettringite. The increase in the intensity of the CH peaks with the curing time, as well as the reduction in the main phases of the alite and belite cement, are evidence of the OPC hydration. 50OPC-30GGBFS-10FA-10GS

composite cement showed a similar behavior than neat OPC, with an increase in the CH content with the curing time. This is not in line with the commonly reported pozzolanic behavior; nevertheless, GGBFS has a higher affinity for the SS activator than for the CH produced by the OPC. Reduced CS values for this system are consistent with previously reported publications [26,47]. The pozzolanic effect of GS and FA showed a reduction in the CH compared to neat OPC, but without a reduction during the time.

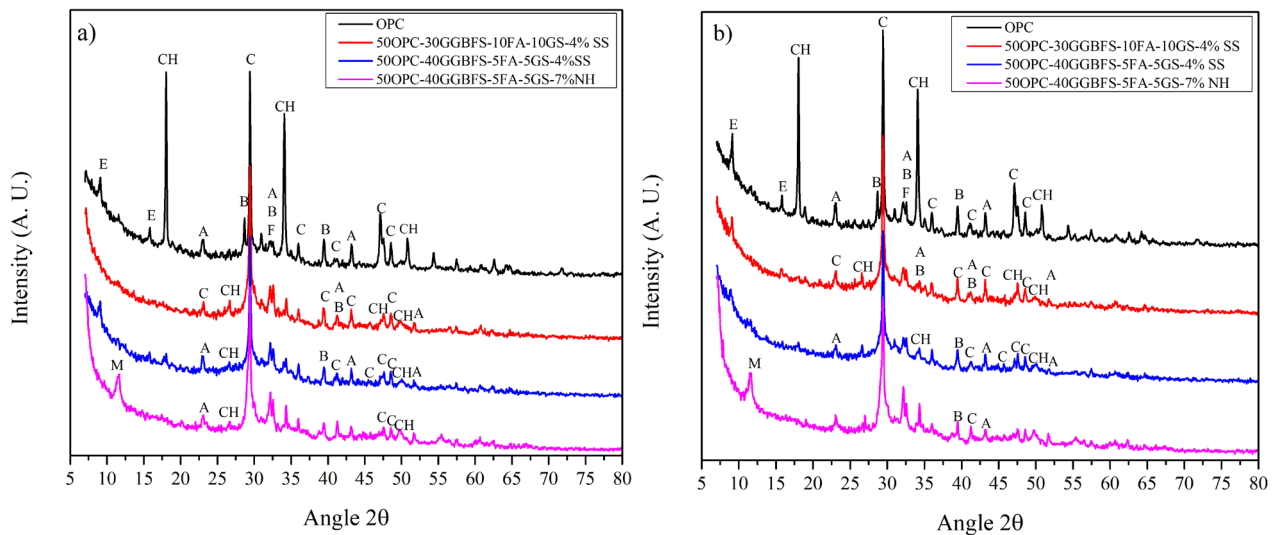


Figure 5. XRD diffraction patterns of the OPC and composite cements systems of 50OPC-30GGBFS-10FA-10GS, and 50OPC-40GGBFS-5FA-5GS activated with 4% $\text{Na}_2\text{O}_{\text{eq}}$ of SS; and 50OPC-40GGBFS-5FA-5GS, activated with 7% $\text{Na}_2\text{O}_{\text{eq}}$ of NH, cured at (a) 3 and (b) 28 days (E = ettringite, CH = portlandite, A = alite, B = belite, F = ferrite, C = calcite, M = monosulfate).

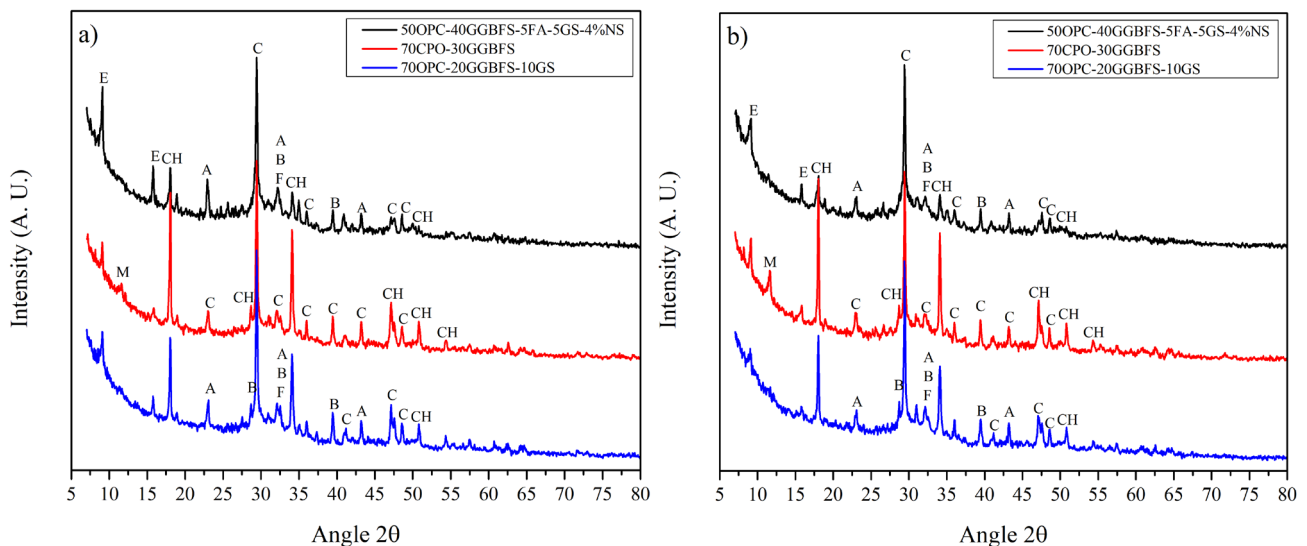


Figure 6. XRD diffraction patterns of the OPC and composite cements systems of 50OPC-40GGBFS-5FA-5GS activated with 4% $\text{Na}_2\text{O}_{\text{eq}}$ of SN; and 70OPC-30GGBFS, 70OPC-20GGBFS-10GS without activator cured at (a) 3 and (b) 28 days (E = ettringite, CH = portlandite, A = alite, B = belite, F = ferrite, C = calcite, M = monosulfate).

Samples with the lowest CS were those activated with NH. Similar results were reported elsewhere for alkaline activated cementitious systems with high GGBFS content [33,60]. Following from that, XRD patterns for 50OPC, 40GGBFS, 5GS, and 5FA activated with 7% $\text{Na}_2\text{O}_{\text{eq}}$ of NH, showed a diminution in the CH at 3 days of curing,

compared to other systems, so it could be said that the OPC was not completely hydrated at 28 days. One of the possible reasons that determines the effectiveness of this activator is that NH could act as a retardant of the hydration of the cement, and at very high levels could produce an indefinite delay. Likewise, there is a detrimental interaction between the external activator (NH) and the OPC; the NH and SCM reaction was also unfavorable. The formation of amorphous gels that contain (N)-S-H could also be detrimental for the systems since those gels could be dissolving into the curing water, due to their instability under saturated conditions. The systems with NS as alkaline activator showed the highest CS, higher than those of OPC. NS is an excellent alkaline activator, but its main disadvantage is that it contains SO_4 , which could lead to the formation of harmful phases in the cement. The 50OPC-40GGBFS-5FA-5GS system contained ettringite as shown by the peak intensities at 9° and $15^\circ 2\theta$. However, the concentration of ettringite did not increase with curing time in this system because it was affected by other factors such as temperature, pH, and sulfate availability. As the curing time progressed, ettringite may have been dissolved or converted to other phases, resulting in a decrease in its concentration after 28 days of hydration. This result is congruent with the CS results where the strengths increased significantly at later ages. A slight decrease in CH is also observed, which could be an indication of the pozzolanic activity of FA and GS.

Regarding the mixes without alkaline activation and lower replacements levels, Figure 2 shows the diffraction pattern of the 70OPC-30GGBFS system, which presented the lowest strength of all the systems without activation. It has been reported that systems with GGBFS show improvements in mechanical properties at long hydration times, since they require the cement to have reacted to begin hydration. As indicated above, the formation of ettringite is observed in the presence of slag, which occurs due to the sulfur contained in it. In addition, there is no evident CH consumption in the XRD patterns, which suggests that at least up to 28 days of curing the GGBFS did not present a hydration reaction as described previously. The 70OPC-20GGBFS-10GS system without activator exhibited the higher mechanical strength among the composites studied, its XRD patterns are shown in Figure 6. These patterns show the presence of AFt at early ages and its disappearance at late ages; Lee, Shi and Day, and Wu and Naik, found that due to the capacity of this phase to increase its volume up to 160%, there is a beneficial effect since it densifies the matrix increasing the RC of the systems, together with the microfiller effect of GS and FA. CH intensity was significantly lower compared to 70OPC-30GGBFS system, which indicates the pozzolanic and synergetic effect of the SCM added. GS has the characteristic of acting as nucleation sites due to its small particle size and its pozzolanic activity, which promotes the formation of new C-S-H gel, greatly benefiting the performance of the system [18,19].

3.3. Thermogravimetric Analysis

This section discusses the curves obtained by TGA of selected composite cements with and without alkaline activation, compared to OPC. The TGA curves show a zone at $200^\circ C$ for OPC and composite cements where free water and some hydration phases such as AFt, AFm, and C-S-H decompose. Subsequently, weight loss observed between $400\text{--}550^\circ C$, corresponds to the CH dehydroxylation process, and finally the decarbonation of the OPC limestone and hydration products carbonation occurs at $600\text{--}800^\circ C$.

Figure 7a shows the TGA curves of the SS activated systems, which showed the best CS, and the NH activated system, which showed the lowest strength values compared to OPC. The SS activated systems showed higher mass loss than the NH-activated system, indicating more hydration products in the former. The NH-activated system had a lower peak intensity than the SS-activated systems, indicating a lower degree of reaction and product formation, demonstrating the consumption of CH by the substitutes. Figure 7b shows the TGA curves for the systems activated with NS, where, as in the previous figure, a clear weight loss due to CH dehydroxylation can be seen, especially in the 50OPC-40GGBFS-5FA-5GS and 50OPC-30GGBFS-10FA-10GS systems compared to the OPC. It can also be observed that the 50OPC-25GGBFS-15FA-10GS system has a lower CH consumption,

which may be due to the higher FA content, which has a lower pozzolanic activity at short hydration times. This phenomenon was confirmed by scanning electron microscopy. For the latter system, the decarbonation zone of the limestone is also more pronounced for OPC and FA. In the case of the non-activated systems in Figure 7c, in the 70OPC-30GGBFS system the CH was completely consumed; this could be due to the slag reaction and the dilution effect due to the lower amount of OPC producing it. In the systems with and without FA, a remarkable consumption of CH was also observed, which is likely to increase with the curing time, proving the pozzolanic effect of the replacement materials.

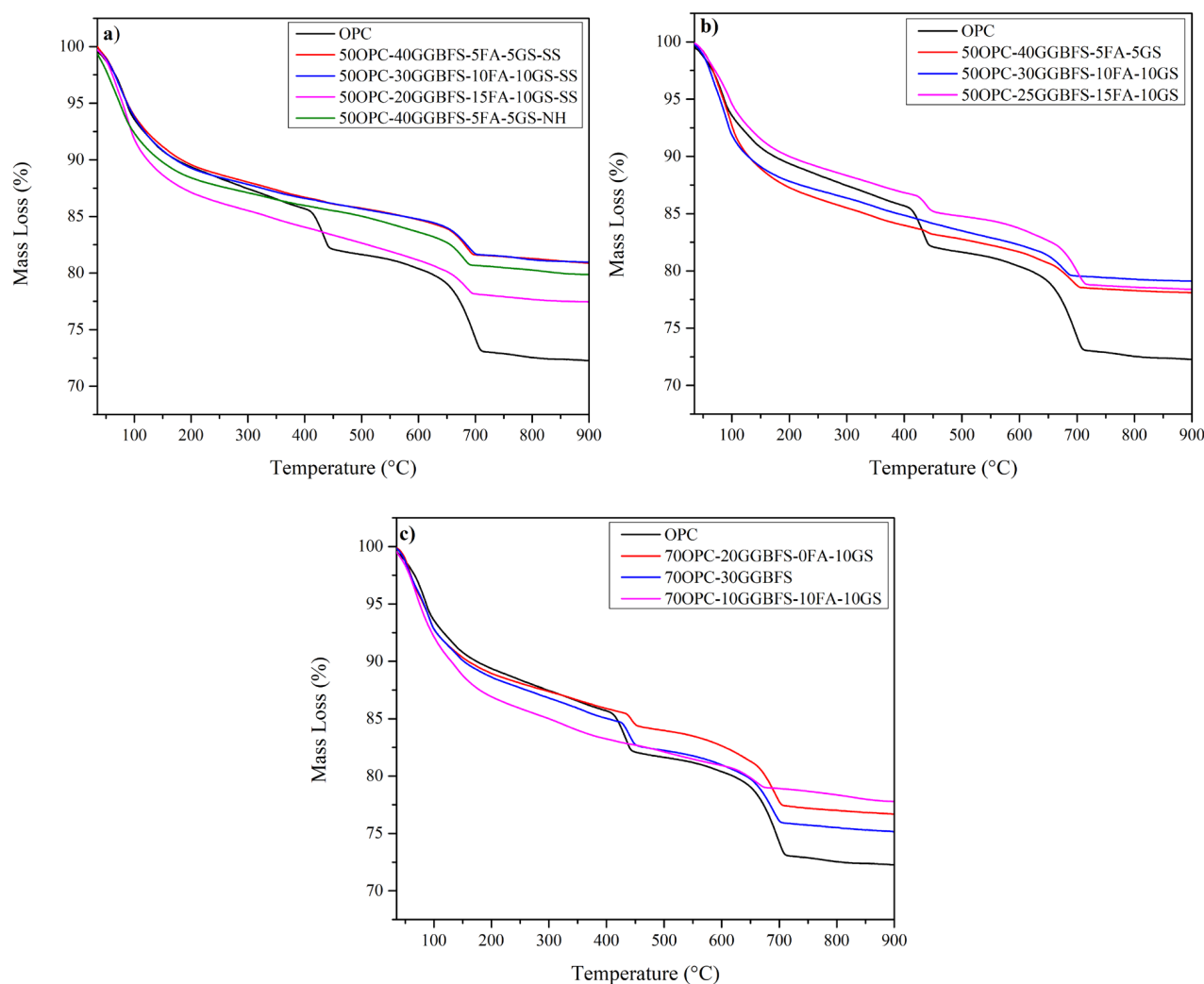


Figure 7. TGA curves of systems cured for 28 days, activated with (a) 4% $\text{Na}_2\text{O}_{\text{eq}}$ of o SS and NH (b) 4% $\text{Na}_2\text{O}_{\text{eq}}$ to SN and (c) without activation.

3.4. Scanning Electron Microscopy and Energy Dispersive X-ray Spectroscopy

Samples from the cementitious systems were selected for representativeness based on the type and amount of alkaline activator and CS results. The micrographs shown are of OPC and partially replaced samples cured for 28 days.

Figure 8 shows the micrographs of the 50OPC-30GGBFS-10FA-10GS system activated with 4% $\text{Na}_2\text{O}_{\text{eq}}$ of SS. It has been reported that one of the best alkaline activators and therefore most used is sodium silicate [31]. The micrograph shows that GGBFS and GS were both activated because they exhibited reaction rings with a different shade of gray, which indicates a hydrated composition. However, there was no reaction ring around the FA particles, which indicates the lack of dissolution and reaction of FA in the environment generated in the system. Different zones of the sample were analyzed with the purpose of

finding FA particles that would demonstrate the interaction with the activator, but they were not found. Some cracking zones were also observed, which could be due to the presence of (N)-S-H and (N)-C-S-H gels, that could be affected by the curing conditions, results from EDS indicated the presence of those types of gels [61].

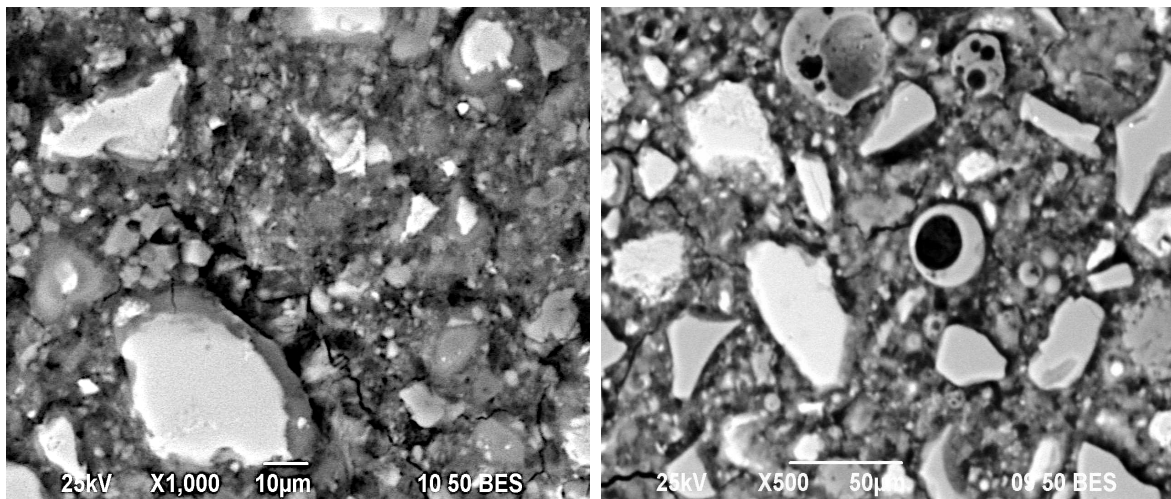


Figure 8. Micrographs of the 50OPC-30GGBFS-10FA-10GS system activated with 4% $\text{Na}_2\text{O}_{\text{eq}}$ of SS cured for 28 days.

Figure 9 is a micrograph of the 50OPC-40GGBFS-5FA-5GS system activated with 4% $\text{Na}_2\text{O}_{\text{eq}}$ to NS, cured for 28 days. The Cs results of the systems activated with this compound show a very favorable behavior even at late ages. GGBFS and GS particles as well as OPC particles have reaction rings, but FA particles did not. The presence of ettringite was also found in the systems, confirming the results obtained by XRD.

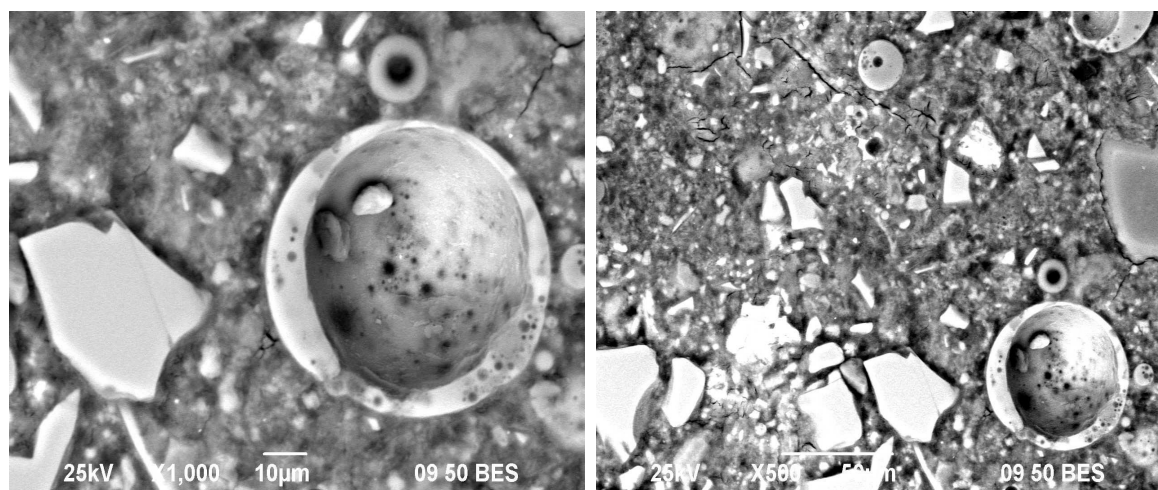


Figure 9. Micrographs of the 50OPC-40GGBFS-5FA-5GS system activated with 4% $\text{Na}_2\text{O}_{\text{eq}}$ of SN cured for 28 days.

Since the systems activated with NH showed a significant deterioration in mechanical properties compared to OPC, the effect of this activator on the matrix of the composite cements was monitored. Figure 10 shows that in the systems activated with NH, no reaction rings can be seen around the particles of the substitute materials; however, the damage to the cementitious matrix is very noticeable. This confirms the selective effect of the alkaline activator proposed by Hooton et al., [62] and there are several cracks with different sizes scattered throughout the sample, due to the presence of non-stable gels.

Two NH-activated systems (50OPC-25GGBFS-15FA-10GS and 50OPC-40GGBFS-5FA-5GS) were analyzed by SEM in order to compare the two matrices and to try to find the causes of the poor CS development of these systems, concluding that an excessive attack on the cement grains occurred, a total absence of interaction of the activator with the grains of the substitute cementitious material, since all the NH was concentrated on retarding the hydration reactions of the cement and promoting the formation of additional gels [63].

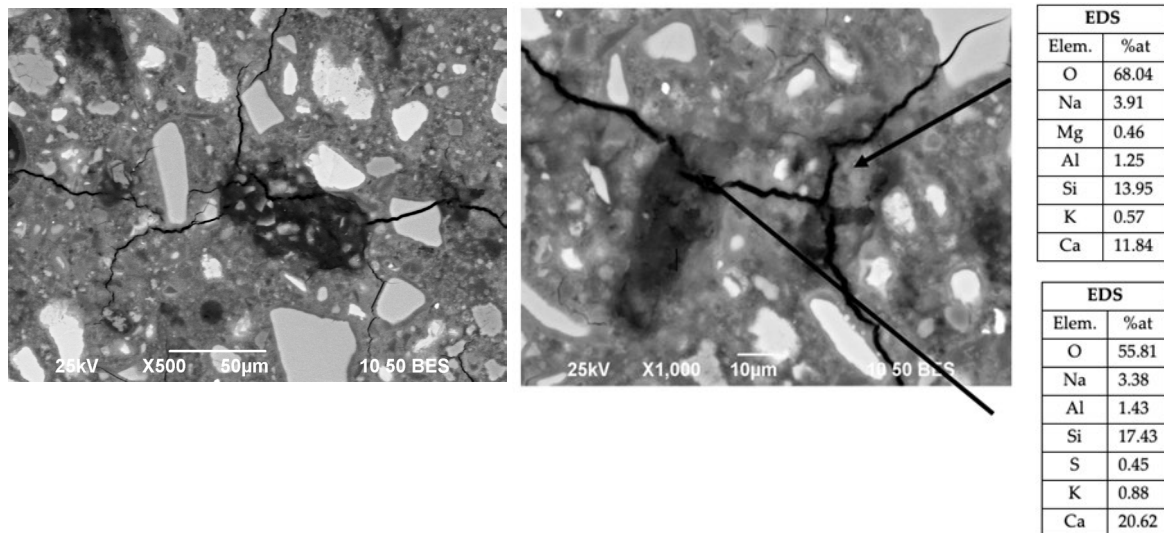


Figure 10. Micrographs of the 50OPC-25GGBFS-15FA-10GS system activated with 7% $\text{Na}_2\text{O}_{\text{eq}}$ of NH cured at 28 days.

As for the mixtures with lower replacement levels, Figure 11 shows the morphology of the 70OPC-10GGBFS-10FA-10GS system without external alkaline activation, which shows hydration products characteristic of an OPC, in addition to edges of different shades of gray around the GGBFS and GS grains, which corresponds to what was obtained in other characterization techniques; however, again the FA grains do not show such surrounding halos that would prove their interaction with the CH generated during the hydration of the cement.

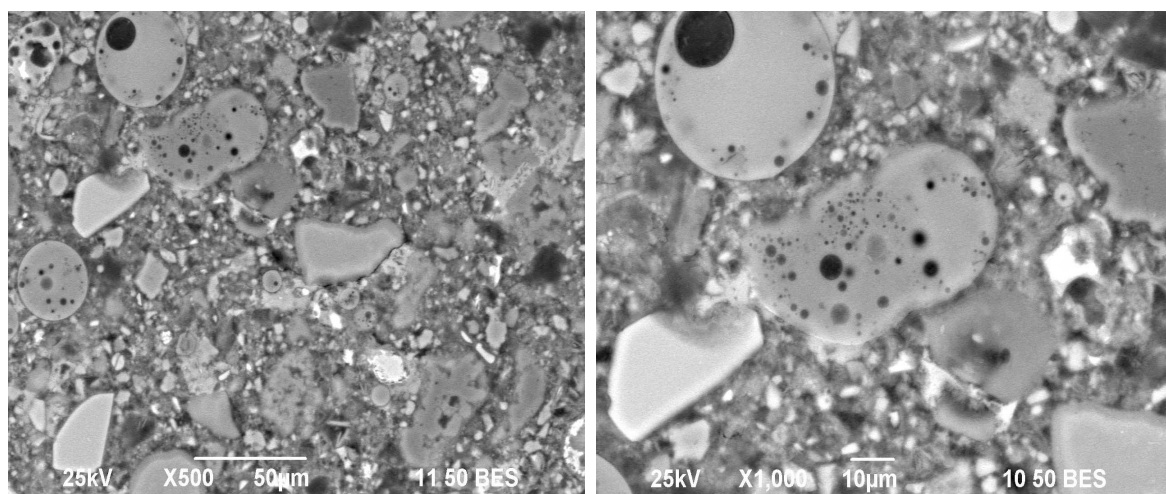


Figure 11. Micrographs of the 70OPC-10GGBFS-10FA-10GS system without activator at cured for 28 days.

3.5. General Discussion

The purpose of this research was to investigate the effects of partially replacing OPC with industrial by-products from various sources to obtain a cementitious composite material with similar or superior properties. One of the most important points was to determine the optimum proportion of materials that would allow for the proposed objectives to be achieved. Another fundamental point was the need to use or not to use an alkaline activator that would be able to react with the SCM involved. The optimal ratio of these activators was determined to be 4% $\text{Na}_2\text{O}_{\text{eq}}$ based on the experimental results and the analysis of the hydration products. The sodium sulfate and sodium silicate activators enhanced the strength development and reduced the porosity of some alkali-activated systems [62]. The results obtained by Criado and cols [64], in alkaline activation of FA with sodium sulfate, indicated that the mechanical strengths and the degree of reaction decreased after 7 days of hydration. This may be due to the fact that this activator does not offer the necessary pH value, concluding that the presence of sodium sulfate did not affect the nature of the reaction products that precipitate during the alkaline activation process. Moreover, other authors [65], observed that in hybrid cements, the presence of sodium sulfate can activate the fly ash satisfactorily without affecting the hydration of Portland clinker and setting times were shorter than using another activator. In addition, the hydration of the alite phase (C_3S) was improved, increasing the mechanical strength. NH showed the less effectiveness due to the formation of N-S-H and (N)-C-S-H that could be dissolved into the curing environment (calcium hydroxide saturated water) [61,63,66,67]. The effectiveness of NS was superior to SS based on the ability of both to release the Na^+ ion, which could act as a network modifier in the hydration gel, which depends on the ability of the activator to dissolve in the mixing water and the subsequent release of the ion of interest. NS can promote the formation of late ettringite, which could cause expansion and, in some cases, cracking; however, at early ages it is possible that the expansion produced causes densification of the cementitious matrix, reducing the presence of very large pores and, in the best case, leading to the elimination of porosity or the presence of smaller pores [30].

An important point of discussion is the effect of each of the replacement materials on the cementitious matrix of the systems analyzed in this work.

- Granulated blast-furnace slag. High levels of slag replacement reduced the workability of the pastes due to their morphology. It was confirmed that it prolonged the setting time of the pastes and that the best strengths were obtained at late curing periods (between 14 and 28 days) [44]. The presence of GS was necessary to increase the RC of the systems. The reacted slag promoted the formation of more C-S-H gel responsible for the hardening of the pastes. Partially reacted slag grains were found at 90 days, indicating that an increase in strength could be expected at later ages.
- Fly ash. One of the main advantages of using fly ash is the ability to improve the flowability of the pastes due to its plasticizing properties resulting from its spherical morphology. According to SEM observations, there was no contribution to form C-S-H gel, as there was no interaction between this material and the alkaline activators used. Although the ash did not react as expected, its presence was not trivial, since it promoted the reduction in the porosity of the cementitious matrices (microfiller effect), due to its variety of sizes and spherical shapes [14,15].
- Geothermal silica. Due to its nanometric size, there was a significant improvement in the reduction in porosity [18–20].

4. Conclusions

The main findings resulting from the alkaline activation of composite cements and the comparison of those binders without activation are outlined below:

- Three of the most common alkaline activators (Na_2SiO_3 , NaOH , and Na_2SO_4) were analyzed, with Na_2SO_4 having the best compressive strength results. This behavior could be due to two fundamental aspects: the promotion and acceleration of the

- pozzolanic reaction and the formation of more ettringite (AFt) at early ages that densified the matrix.
- Class F fly ash could not be alkaline activated; however, its presence significantly improved the workability of the pastes and acted as a microfiller helping to reduce the porosity of the cementitious matrices.
 - High volumes of slag significantly reduced the early age strength of the composites, obtaining the best strengths at later ages.
 - The NaOH activator, by increasing the pH of the pastes, promoted the release of alkalis that favored the presence of the (N)-S-H gel. The inability to act as an alkaline activator of partially replaced systems evaluated in this research could be due to a retardation of the Portland cement hydration.
 - Likewise, 30% replaced systems, obtained in the same way positive results using a combination of granulated blast furnace slag and low proportions of geothermal silica and fly ash.
 - There was a significant improvement in the reduction in porosity, with the use of GS, the pozzolanic reaction was observed by XRD and TGA. When also adding GGBFS the results were improved in both systems, with and without activation.

5. Future Works

The replacement of OPC by more than 50% with SCMs, GS, and alkaline activation will lead to economic and environmental benefits, so for future works the reduction in OPC content should be emphasized. The hybrid cement utilizing GS, SCMs, and OPC will be innovative, giving good CS values and less CO₂ emission. Hence, an investigation focusing on the strength and microstructural studies of hybrid cement using GS would attract the attention of the scientific and industrial communities that produce electrical energy from underground sources.

Supplementary Materials: The following supporting information can be downloaded at: <https://www.mdpi.com/article/10.3390/buildings13071854/s1>, Table S1: Compressive strength results activated with 4% of Na₂O_{eq}, compared to OPC; Table S2: Compressive strength results activated with 4% of Na₂O_{eq}, compared to OPC.

Author Contributions: Conceptualization: A.S.M., L.I.R.-B. and L.Y.G.-Z.; materials, methodology, and characterization, A.S.M., L.I.R.-B. and L.Y.G.-Z.; discussion, A.S.M., L.I.R.-B., F.C.F., J.C.-C. and L.Y.G.-Z.; writing—original paper preparation, A.S.M., L.I.R.-B., F.C.F., J.C.-C. and L.Y.G.-Z.; writing—review and editing, results, and discussion, A.S.M., L.I.R.-B., F.C.F., J.C.-C. and L.Y.G.-Z.; visualization—all figures, A.S.M., L.I.R.-B. and L.Y.G.-Z.; project administration, L.Y.G.-Z.; funding acquisition, L.Y.G.-Z. All authors have read and agreed to the published version of the manuscript.

Funding: This research was funded by CONAHCYT (National Council of Humanities, Science and Technology, Consejo Nacional de Humanidades, Ciencia y Tecnología—México) and UANL (PAICYT).

Data Availability Statement: Not applicable.

Acknowledgments: The authors acknowledge full financial support for this research provisioned by the National Council of Humanities, Science and Technology (CONAHCYT-Mexico) and UANL (PAICYT). This research was conducted at FIME-UANL, the authors acknowledge the support that has made the laboratory and the operation possible; to Universidad Nacional de Colombia, and María Zambrano (UPV, Ministry of Universities, Recovery, Transformation, and Resilience Plan—Funded by the European Union—Next Generation EU) of the Institute of Materials Technology of the Polytechnic University of Valencia (Spain); and UPV's Aid to Promote Postdoctoral Research (PAIDPD-22).

Conflicts of Interest: The authors declare no conflict of interest. The founders had no role in the design of the study; in the collection, analyses, or interpretation of data; in the writing of the manuscript; or in the decision to publish the results.

References

1. UN Environment; Scrivener, K.L.; John, V.M.; Gartner, E.M. Eco-efficient cements: Potential economically viable solutions for a low-CO₂ cement-based materials industry. *Cem. Concr. Res.* **2018**, *114*, 2–26. [[CrossRef](#)]
2. Miller, S.A.; John, V.M.; Pacca, S.A.; Horvath, A. Carbon dioxide reduction potential in the global cement industry by 2050. *Cem. Concr. Res.* **2018**, *114*, 115–124. [[CrossRef](#)]
3. Mindess, S.; Young, F.; Darwin, D. *Concrete*, 2nd ed.; Prentice Hall: Upper Saddle River, NJ, USA, 2003.
4. Neville, A.M.; Brooks, J.J. *Concrete Technology*, 2nd ed.; Prentice Hall: Upper Saddle River, NJ, USA, 2010.
5. Montoya, A.S.; Chung, C.-W.; Kim, J.-H. High Performance Concretes with Highly Reactive Rice Husk Ash and Silica Fume. *Materials* **2023**, *16*, 3903. [[CrossRef](#)] [[PubMed](#)]
6. Ludwig, H.-M.; Zhang, W. Research review of cement clinker chemistry. *Cem. Concr. Res.* **2015**, *78*, 24–37. [[CrossRef](#)]
7. Worrell, E.; Price, L.; Martin, N.; Hendriks, C.; Meida, L.O. Carbon dioxide emission from global cement industry. *Annu. Rev. Energy Environ.* **2001**, *26*, 303–329. [[CrossRef](#)]
8. Robayo-Salazar, R.; Mejía-Arcila, J.; de Gutiérrez, R.M.; Martínez, E. Life cycle assessment (LCA) of an alkali-activated binary concrete based on natural volcanic pozzolan: A comparative analysis to OPC concrete. *Constr. Build. Mater.* **2018**, *176*, 103–111. [[CrossRef](#)]
9. Qin, L.; Gao, X.; Li, Q. Upcycling carbon dioxide to improve mechanical strength of Portland cement. *J. Clean. Prod.* **2018**, *196*, 726–738. [[CrossRef](#)]
10. Escalante-García, J.I.; Magallanes-Rivera, R.X.; Gorokhovskiy, A. Waste gypsum–blast furnace slag cement in mortars with granulated slag and silica sand as aggregates. *Constr. Build. Mater.* **2009**, *23*, 2851–2855. [[CrossRef](#)]
11. Van den Heede, P.; De Belie, N. Environmental impact and life cycle assessment (LCA) of traditional and ‘green’ concretes: Literature review and theoretical calculations. *Cem. Concr. Compos.* **2012**, *34*, 431–442. [[CrossRef](#)]
12. Saha, A.K.; Khan, M.; Sarker, P.K. Value added utilization of by-product electric furnace ferronickel slag as construction materials: A review. *Resour. Conserv. Recycl.* **2018**, *134*, 10–24. [[CrossRef](#)]
13. Gartner, E.M.; Macphee, D.E. A physico-chemical basis for novel cementitious binders. *Cem. Concr. Res.* **2011**, *41*, 736–749. [[CrossRef](#)]
14. Snellings, R.; Mertens, G.; Elsen, J. Supplementary Cementitious Materials. *Rev. Miner. Geochem.* **2012**, *74*, 211–278. [[CrossRef](#)]
15. Lothenbach, B.; Scrivener, K.; Hooton, R. Supplementary cementitious materials. *Cem. Concr. Res.* **2011**, *41*, 1244–1256. [[CrossRef](#)]
16. Aitcin, P.-C. Supplementary cementitious materials and blended cements. In *Science and Technology of Concrete Admixtures*; Elsevier: Amsterdam, The Netherlands, 2016; pp. 53–73. [[CrossRef](#)]
17. Das, B.; Prakash, S.; Reddy, P.S.R.; Misra, V.N. An overview of utilization of slag and sludge from steel industries. *Resour. Conserv. Recycl.* **2007**, *50*, 40–57. [[CrossRef](#)]
18. Iñiguez-Sánchez, C.; Gómez-Zamorano, L.; Alonso, M. Impact of nano-geothermal silica waste and chloride content on pore solution, microstructure, and hydration products in Portland cement pastes. *J. Mater. Sci.* **2012**, *47*, 3639–3647. [[CrossRef](#)]
19. Gómez-Zamorano, L.Y.; Escalante-García, J.I.; Mendoza-Suárez, G. Geothermal waste: An alternative replacement material of portland cement. *J. Mater. Sci.* **2004**, *39*, 4021–4025. [[CrossRef](#)]
20. Escalante, J.; Mendoza, G.; Mancha, H.; López, J.; Vargas, G. Pozzolanic properties of a geothermal silica waste material. *Cem. Concr. Res.* **1999**, *29*, 623–625. [[CrossRef](#)]
21. John, V.M.; Damineli, B.L.; Quattrone, M.; Pileggi, R.G. Fillers in cementitious materials—Experience, recent advances and future potential. *Cem. Concr. Res.* **2018**, *114*, 65–78. [[CrossRef](#)]
22. Bijen, J. Benefits of slag and fly ash. *Constr. Build. Mater.* **1996**, *10*, 309–314. [[CrossRef](#)]
23. Jamali, M.; Gupta, S. Utilization of silica fume with fly ash and properties of Portland cement-silica fume-fly ash-concrete. *AIP Conf. Proc.* **2023**, *2558*, 020025. [[CrossRef](#)]
24. Li, X.; Bai, C.; Qiao, Y.; Wang, X.; Yang, K.; Colombo, P. Preparation, properties and applications of fly ash-based porous geopolymers: A review. *J. Clean. Prod.* **2022**, *359*, 132043. [[CrossRef](#)]
25. Barboza-Chavez, A.C.; Gómez-Zamorano, L.Y.; Acevedo-Dávila, J.L. Synthesis and Characterization of a Hybrid Cement Based on Fly Ash, Metakaolin and Portland Cement Clinker. *Materials* **2020**, *13*, 1084. [[CrossRef](#)] [[PubMed](#)]
26. Zhao, F.-Q.; Ni, W.; Wang, H.-J.; Liu, H.-J. Activated fly ash/slag blended cement. *Resour. Conserv. Recycl.* **2007**, *52*, 303–313. [[CrossRef](#)]
27. García-Lodeiro, I.; Fernández-Jiménez, A.; Palomo, A. Variation in hybrid cements over time. Alkaline activation of fly ash–portland cement blends. *Cem. Concr. Res.* **2013**, *52*, 112–122. [[CrossRef](#)]
28. Amran, M.; Murali, G.; Khalid, N.H.A.; Fediuk, R.; Ozbakkaloglu, T.; Lee, Y.H.; Haruna, S.; Lee, Y.Y. Slag uses in making an ecofriendly and sustainable concrete: A review. *Constr. Build. Mater.* **2021**, *272*, 121942. [[CrossRef](#)]
29. García-Lodeiro, I.; Fernández-Jiménez, A.; Palomo, A. Cementos híbridos de bajo impacto ambiental: Reducción del factor Clinker. *Rev. ALCONPAT* **2015**, *5*, 1–17. [[CrossRef](#)]
30. Guerra-Cossío, M.A.; González-López, J.R.; Magallanes-Rivera, R.X.; Zaldívar-Cadena, A.A.; Figueroa-Torres, M.Z. Anhydrite, blast-furnace slag and silica fume composites: Properties and reaction products. *Adv. Cem. Res.* **2019**, *31*, 362–369. [[CrossRef](#)]
31. Shi, C.; Roy, D.; Krivenko, P. *Alkali-Activated Cements and Concretes*; CRC Press: Boca Raton, FL, USA, 2003. [[CrossRef](#)]
32. Luukkonen, T.; Abdollahnejad, Z.; Yliniemi, J.; Kinnunen, P.; Illikainen, M. One-part alkali-activated materials: A review. *Cem. Concr. Res.* **2018**, *103*, 21–34. [[CrossRef](#)]

33. Wang, S.-D.; Scrivener, K.L.; Pratt, P. Factors affecting the strength of alkali-activated slag. *Cem. Concr. Res.* **1994**, *24*, 1033–1043. [[CrossRef](#)]
34. Batuecas, E.; Ramón-Álvarez, I.; Sánchez-Delgado, S.; Torres-Carrasco, M. Carbon footprint and water use of alkali-activated and hybrid cement mortars. *J. Clean. Prod.* **2021**, *319*, 128653. [[CrossRef](#)]
35. Palomo, A.; Krivenko, P.V.; Garcia-Lodeiro, I.; Kavalerova, E.; Maltseva, O.; Fernández-Jimenez, A.M. A review on alkaline activation: New analytical perspectives. *Mater. Constr.* **2014**, *64*, e022. [[CrossRef](#)]
36. Dacić, A.; Kopecskó, K.; Fenyvesi, O.; Merta, I. The Obstacles to a Broader Application of Alkali-Activated Binders as a Sustainable Alternative—A Review. *Materials* **2023**, *16*, 3121. [[CrossRef](#)] [[PubMed](#)]
37. Sun, X.; Zhao, Y.; Qiu, J.; Xing, J. Review: Alkali-activated blast furnace slag for eco-friendly binders. *J. Mater. Sci.* **2022**, *57*, 1599–1622. [[CrossRef](#)]
38. Redden, R.; Neithalath, N. Microstructure, strength, and moisture stability of alkali activated glass powder-based binders. *Cem. Concr. Compos.* **2014**, *45*, 46–56. [[CrossRef](#)]
39. Qu, B.; Martin, A.; Pastor, J.; Palomo, A.; Fernández-Jiménez, A. Characterisation of pre-industrial hybrid cement and effect of pre-curing temperature. *Cem. Concr. Compos.* **2016**, *73*, 281–288. [[CrossRef](#)]
40. Fernández-Jiménez, A.; Palomo, A.; Sobrados, I.; Sanz, J. The role played by the reactive alumina content in the alkaline activation of fly ashes. *Microporous Mesoporous Mater.* **2006**, *91*, 111–119. [[CrossRef](#)]
41. Rivera, J.F.; Mejia, J.M.; de Gutierrez, R.M.; Gordillo, M. Hybrid cement based on the alkali activation of by-products of coal. *Rev. Constr.* **2014**, *13*, 31–39. [[CrossRef](#)]
42. Sánchez-Herrero, M.J.; Fernández-Jiménez, A.; Palomo, A. Studies about the Hydration of Hybrid “Alkaline-Belite” Cement. *Front. Mater.* **2019**, *6*, 66. [[CrossRef](#)]
43. Lodeiro, I.G.; Macphée, D.; Palomo, A.; Fernández-Jiménez, A. Effect of alkalis on fresh C–S–H gels. FTIR analysis. *Cem. Concr. Res.* **2009**, *39*, 147–153. [[CrossRef](#)]
44. Escalante, J.; Gómez, L.; Johal, K.; Mendoza, G.; Mancha, H.; Méndez, J. Reactivity of blast-furnace slag in Portland cement blends hydrated under different conditions. *Cem. Concr. Res.* **2001**, *31*, 1403–1409. [[CrossRef](#)]
45. Gutteridge, W.A.; Dalziel, J.A. Filler cement: The effect of the secondary component on the hydration of Portland cement: Part 2: Fine hydraulic binders. *Cem. Concr. Res.* **1990**, *20*, 853–861. [[CrossRef](#)]
46. Taylor, H.F.W.; Mohan, K.; Moir, G.K. Analytical Study of Pure and Extended Portland Cement Pastes: II, Fly Ash- and Slag-Cement Pastes. *J. Am. Ceram. Soc.* **1985**, *68*, 685–690. [[CrossRef](#)]
47. Liu, S.; Han, W.; Li, Q. Hydration Properties of Ground Granulated Blast-Furnace Slag (GGBS) Under Different Hydration Environments. *Mater. Sci.* **2017**, *23*, 70–77. [[CrossRef](#)]
48. Escalante-García, J.I.; Palacios-Villanueva, V.M.; Gorokhovskiy, A.V.; Mendoza-Suárez, G.; Fuentes, A.F. Characteristics of a NaOH-Activated Blast Furnace Slag Blended with a Fine Particle Silica Waste. *J. Am. Ceram. Soc.* **2004**, *85*, 1788–1792. [[CrossRef](#)]
49. Barnett, S.; Soutsos, M.; Millard, S.; Bungey, J. Strength development of mortars containing ground granulated blast-furnace slag: Effect of curing temperature and determination of apparent activation energies. *Cem. Concr. Res.* **2006**, *36*, 434–440. [[CrossRef](#)]
50. Salas, A.; Delvasto, S.; de Gutiérrez, R.M. Developing high-performance concrete incorporating highly-reactive rice husk ash. *Ing. Investig.* **2013**, *33*, 49–55. [[CrossRef](#)]
51. *ASTM C109/C109M-20*; Standard Test Method for Compressive Strength of Hydraulic Cement Mortars (Using 2-in. or [50-mm] Cube Specimens). ASTM: Philadelphia, PA, USA, 2020.
52. Maciel, M.H.; Soares, G.S.; de Oliveira Romano, R.C.; Cincotto, M.A. Monitoring of Portland cement chemical reaction and quantification of the hydrated products by XRD and TG in function of the stoppage hydration technique. *J. Therm. Anal. Calorim.* **2019**, *136*, 1269–1284. [[CrossRef](#)]
53. Chi, L.; Wang, Z.; Lu, S.; Zhao, D.; Yao, Y. Development of mathematical models for predicting the compressive strength and hydration process using the EIS impedance of cementitious materials. *Constr. Build. Mater.* **2019**, *208*, 659–668. [[CrossRef](#)]
54. Zeghichi, L.; Mezghiche, B.; Chebili, R. Study of the effect of alkalis on the slag cement systems. *Can. J. Civ. Eng.* **2005**, *32*, 934–939. [[CrossRef](#)]
55. Shi, C.; Day, R.L. Pozzolanic reaction in the presence of chemical activators: Part II—Reaction products and mechanism. *Cem. Concr. Res.* **2000**, *30*, 607–613. [[CrossRef](#)]
56. Palomo, A.; Jimenez, A.M.F.; Kovalchuk, G.; Ordoñez, L.M.; Naranjo, M.C. Opc-fly ash cementitious systems: Study of gel binders produced during alkaline hydration. *J. Mater. Sci.* **2007**, *42*, 2958–2966. [[CrossRef](#)]
57. Hewlett, P.C. (Ed.) *Lea’s Chemistry of Cement and Concrete*; Elsevier: Amsterdam, The Netherlands, 1998. [[CrossRef](#)]
58. Barnes, P.; Bensted, J. *Structure and Performance of Cements*; CRC Press: Boca Raton, FL, USA, 2002. [[CrossRef](#)]
59. Escalante-García, J.I.; Gorokhovskiy, A.V.; Mendoza, G.; Fuentes, A. Effect of geothermal waste on strength and microstructure of alkali-activated slag cement mortars. *Cem. Concr. Res.* **2003**, *33*, 1567–1574. [[CrossRef](#)]
60. Fernández-Jiménez, A.; Palomo, J.; Puertas, F. Alkali-activated slag mortars: Mechanical strength behaviour. *Cem. Concr. Res.* **1999**, *29*, 1313–1321. [[CrossRef](#)]
61. Mashizi, M.N.; Bagheripour, M.H.; Jafari, M.M.; Yaghoubi, E. Mechanical and Microstructural Properties of a Stabilized Sand Using Geopolymer Made of Wastes and a Natural Pozzolan. *Sustainability* **2023**, *15*, 2966. [[CrossRef](#)]
62. Hooton, R.; Shi, C.; Day, R. Selectivity of Alkaline Activators for the Activation of Slags. *Cem. Concr. Aggregates* **1996**, *18*, 8–14. [[CrossRef](#)]

63. Nicoara, A.I.; Badanoiu, A.I. Influence of Alkali Activator Type on the Hydrolytic Stability and Intumescence of Inorganic Polymers Based on Waste Glass. *Materials* **2021**, *15*, 147. [[CrossRef](#)]
64. Criado, M.; Jiménez, A.F.; Palomo, A. Effect of sodium sulfate on the alkali activation of fly ash. *Cem. Concr. Compos.* **2010**, *32*, 589–594. [[CrossRef](#)]
65. Donatello, S.; Fernández-Jimenez, A.; Palomo, A. Very High Volume Fly Ash Cements. Early Age Hydration Study Using Na₂SO₄ as an Activator. *J. Am. Ceram. Soc.* **2013**, *96*, 900–906. [[CrossRef](#)]
66. Dave, S.V.; Bhogayata, A.; Arora, N.K. Mix design optimization for fresh, strength and durability properties of ambient cured alkali activated composite by Taguchi method. *Constr. Build. Mater.* **2021**, *284*, 122822. [[CrossRef](#)]
67. Dave, S.V.; Bhogayata, A. The strength oriented mix design for geopolymer concrete using Taguchi method and Indian concrete mix design code. *Constr. Build. Mater.* **2020**, *262*, 120853. [[CrossRef](#)]

Disclaimer/Publisher's Note: The statements, opinions and data contained in all publications are solely those of the individual author(s) and contributor(s) and not of MDPI and/or the editor(s). MDPI and/or the editor(s) disclaim responsibility for any injury to people or property resulting from any ideas, methods, instructions or products referred to in the content.